Straightforward access to multifunctional π-conjugated P-heterocycles

Thomas Delouche,[a] Elsa Caytan, [a] Marie Cordier, [a] Thierry Roisnel,[a] Grégory Taupier,[a] Yann Molard, [a] Nicolas Vanthuyne,[b] Boris Le Guennic,[a] Muriel Hissler,[a] Denis Jacquemin,[c] and Pierre-Antoine Bouit [a]

a Univ Rennes, CNRS, ISCR – UMR 6226, ScanMAT – UMS 2001, Rennes F-35000, France. E-mail : pierre-antoine.bouit@univ-rennes1.fr

b Aix Marseille Univ, CNRS, Centrale Marseille, iSm2, Marseille, France

c CEISAM Lab-UMR 6230, CNRS, Nantes University, Nantes, France. E-mail : denis.jacquemin@univ-nantes.fr

Abstract: We report the straightforward one-pot synthesis of 5 or 6-membered P-heterocycles featuring internal ylidic bond: P-containing acenaphthylenes and phenanthrenes. The stability of the compounds tolerates post-functionalization through direct arylation to introduce electron-rich/poor substituents and the synthetic strategy is also compatible with the preparation of more elaborated polyaromatic scaffolds such acenes and helicenes. Using a joint experimental and theoretical approach, we show that the molecular engineering of this platform allows not only tuning their absorption/emission on the entire visible range but also endowing them with chiroptical or non-linear optical properties, making them valuable dyes for a large panel of photonic or opto-electronic applications.

In the blooming field of functional materials based on organophosphorus π-conjugated heterocycles,[1][2][3][4] little attention has been devoted to phosphacycles featuring internal λ^5-P-C bond. Such ylidic bond was supposed to be too reactive yet its ability to efficiently delocalize charges was discussed.[5] However, various recent reports on the properties of π-extended λ^5-phosphinines (also called phosphabenzene) shed a new light on this “old” heterocycle.[6][7] In these systems, the bonding topology can be described as a combination between two limit forms: (i) a Hückel type aromatic system and (ii) a cyclic phosphonium ylide with a negatively charged carbon backbone (**A**, Fig 1). The intense fluorescence of its π-extended form, associated with remarkable chemical and thermal stability allowed using it as emitter in OLED or in organic laser (**B**, Fig 1).[8][9][10][11] Regarding five-membered ring, limited reports describe the properties of λ^5-phospholes or diphospha-acenes such **C** (Fig. 1).[12][13] In these systems also, the bonding topology results from a combination of resonant forms. Although these recent results highlighted the promising optical and redox properties of these “ylidic” P-heterocycles in the context molecular electronics and photonics, efficient synthetic methods to prepare them remain limited.[14][15][16][17][18][19][20]

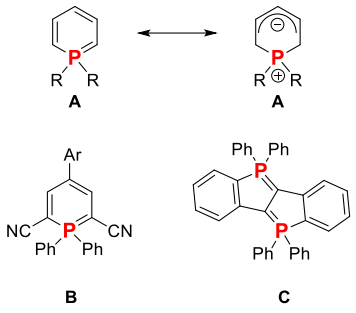

Figure 1: Resonant form of λ^5-phosphinine **A**, representative examples of π-extended λ^5-phosphinines **B**, examples of 5-membered P-ring with internal λ^5-P-C bond (**C**).

In this article, we report a straightforward synthesis that allows obtaining in one-pot P-containing acenaphthylenes or phenanthrenes featuring internal ylidic bond (**E** and **G**, Fig 2). These compounds are easily obtained through intramolecular cyclization of ylides generated from readily available phosphine **D** and **F** (Fig. 2). Such simple heteroaromatics synthesis can be extended to more elaborated P-containing acenes and helicenes. The molecular engineering of this heterocycle allows tuning their

photophysical on the entire visible range as well as their redox properties. These modifications were rationalized using DFT methods. Finally, we could also endow them with chiroptical or non-linear optical properties.

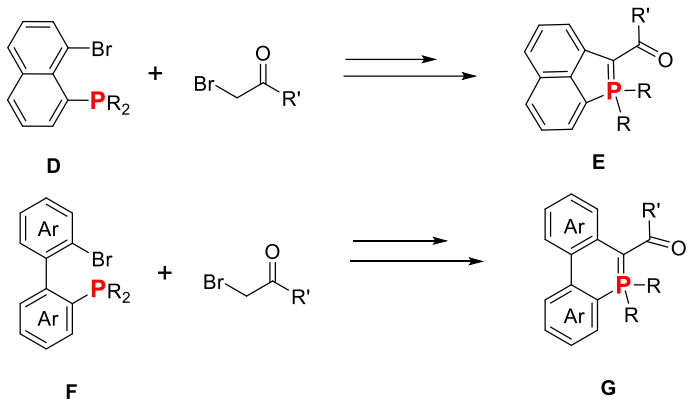

Figure 2: Synthesis of 5 or 6-membered P-heterocycles featuring internal λ^5-P-C bond **E** and **G**.

Synthesis. During our study of the reactivity of bromo-naphthyl phosphine such as **1a** (Scheme 1), we observed that refluxing carbonyl-stabilized phosphonium ylide **4a** (^{31}P NMR = + 23.8 ppm) in toluene leads to an intramolecular cyclization with the formation of the λ^5-phosphaacenaphthylene **5a** in good yields (52 %, ^{31}P NMR = + 22.8 ppm).[21] **5a** was fully characterized by multinuclear NMR spectroscopy and MS analysis. In particular, the typical ^{13}C shift of carbonyl is observed (δ = 185.7 ppm). **5a** is fully air and moisture stable and can be purified through chromatography on silica. In addition, **5a** was characterized by single crystal X-ray diffraction (*vide infra*). Related sequence of intramolecular cyclization of an ylide followed by a rearomatization under basic conditions was previously observed by Hayashi *et a*l in their synthesis of 3-oxo-λ^5 -phosphole.[22] Interestingly, Xu *et al* reported that the Pd-catalysed intramolecular cyclization of related carbonyl-stabilized phosphonium ylides proceed through Ullman-type O-arylation.[23] With our phosphonium, the use of various Pd catalysts ($Pd(PPh_3)_4$, $PdCl_2(PPh_3)_2$, $Pd(OAc)_2$ etc) did not change the fate of the reaction and only the λ^5-phosphaacenaphthylene **5a** was formed in similar yields.

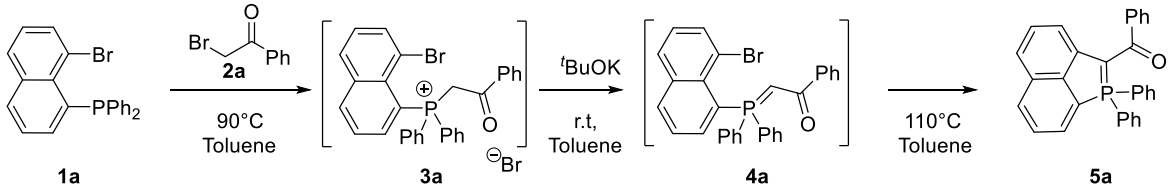

Scheme 1: Synthesis of phosphaacenaphthylene **5a**

In order to study the scope of the reaction, various arylcarbonyl phosphonium ylides were tested (Scheme 2). The reaction efficiently proceeds with electron poor aryl such as **2b-c**. However, no final product was observed in the case of electron rich ^{t}Bu (**2d**) or thienyl (**2e**). Similarly, no reaction occurs if the ylide is not stabilized by a ketone. Finally, the reaction is tolerant to modification of the phosphine as exemplified with the reaction with cyclohexylphosphine (**1b)**. To summarize, such methodology allows easily accessing a family of phosphaacenaphthylene featuring internal ylidic bond. Modifications of the carbonyl substituent as well as the exocyclic P-substituent can be performed.

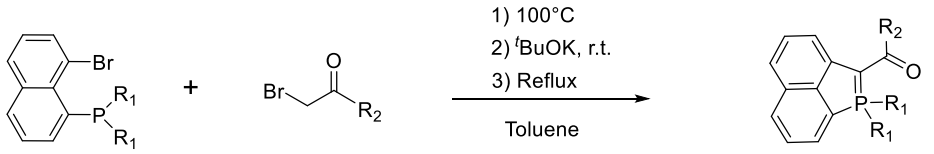

1a. R_1 = Ph
1b. R_1 = Cy

2a : R_2 = Ph
2b : R_2 = 4-$(NO_2)C_6H_4$
2c : R_2 = 3,5-$(CF_3)_2C_6H_3$
2d : R_2 = ^{t}Bu
2e : R_2 = C_4H_4S
2f: R1 = Cy; R_2 = Ph

5a : R_1 = Ph; R_2 = Ph (58%)
5b : R_1 = Ph; R_2 = 4-$(NO_2)C_6H_4$ (70%)
5c : R_1 = Ph; R_2 = 3,5-$(CF_3)_2C_6H_3$ (60%)
5d : R_1 = Ph;R_2 = ^{t}Bu; (0%)
5e : R_1 = Ph;R_2 = C_4H_4S; (0%)
5f: R_1 = Cy; R_2 = Ph (47%)

Scheme 2: Synthesis of phosphaacenaphthylene **5af**

We were then interested in extending this strategy toward the synthesis of 6-membered P-heterocycles such phosphaphenanthrenes.[24],[25] The methodology was tested with 2-(diphenylphosphino)-2'-dibromo-1,1'-biphenyle **6** (Scheme 3). The thermal reaction only worked when the in situ generated ylide is heated at 175°C in DMF. In this case, the λ^5- phosphaphenanthrenes **7a-b** are synthesized in moderated yields. When the reaction is performed under catalytic conditions ($Pd(PPh_3)_4$, 0,05 eq), the reaction proceeds at 115°C. If the biphenyl moiety of **6** is replaced by a dithienyl scaffold (**8**), the reaction efficiently proceeds toward λ^5-dithienophosphinine **9** (58%, Scheme 3). These results demonstrate that our synthetic strategy also allows efficiently preparing 6-membered P-heterocycles.

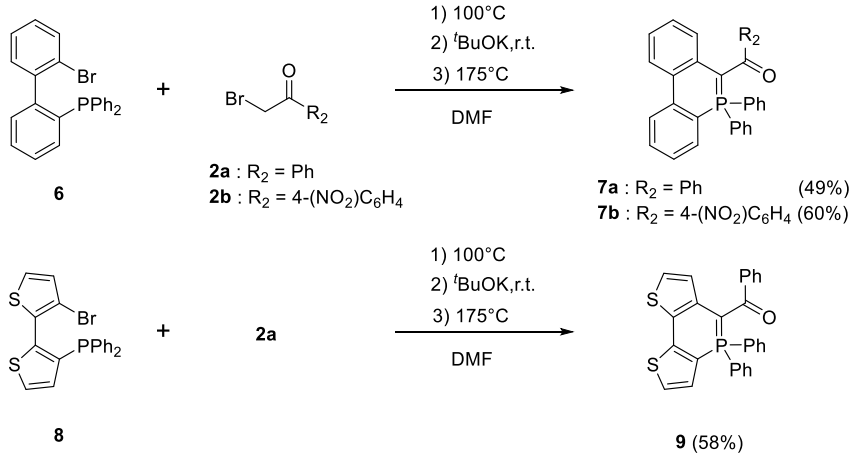

Scheme 3: Synthesis of 6-membered P-heterocycles **7** and **9**

Structural analysis.

Additionally, **5a**, **5b**, **5f**, **7a**, and **9** were also characterized by X-ray diffraction. A detailed inspection is performed below for **5a** that is representative of the entire family (see table S1-2 for details). The polyaromatic platform is fully planar (maximal deviation from mean plane: 0.09 Å) and the P-atom adopts a classical tetrahedral shape. The two intramolecular C-P bonds distances are $d_{P\text{-}C4}$ = 1.75 Å and $d_{P\text{-}C1}$ = 1.79 Å, confirming the ylidic nature of P-C_4 (table S1-2). Similar P-C distances were reported in Hayashi's λ^5-phospholes.[12] Interestingly, the C-C between the λ^5-phosphole and the carbonyl has a distance of 1.42 Å, intermediate between a C-C and C=C, thus illustrating a conjugation between the polyaromatic P-ring and the carbonyl. Finally, a short intramolecular O-P distance is observed (d = 2.90 Å, d_{VdW}(O-P) = 3.32 Å). All these characteristics are constant within the λ^5-phosphaacenaphthene family (Table S2). Regarding the 6-membered P-rings, the general trends are globally the same (Table S2). The main difference is that non-triflling distortion from planarity is observed in the polycyclic framework of **7a** and **9** (maximal deviation from mean plane: 0.17 Å for **9** and 0.40 Å for **7a**). This difference of planarity between **5a** and **7a** is also obvious with DFT calculations (Figure S31), indicating that this is not an effect induced by crystal packing. Finally, this structural analysis confirmed that all compounds display ylidic bond and that the carbonyl group is involved in the conjugated framework. This statement

is confirmed by the frontier molecular orbitals of Figure S31 in which the carbonyl obviously contributes (in the HOMO for **5a**, in both HOMO and LUMO for **7a**).

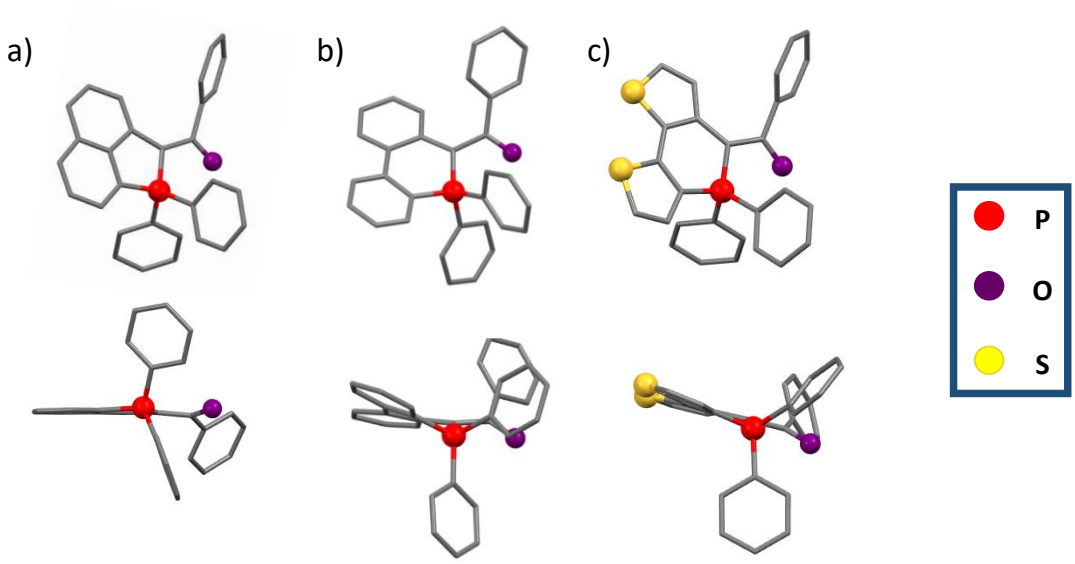

Fig. 3: X-ray structures (top and side view) of (a) **5a**, (b) **7a** and (c) **9**

Optical and redox properties.

The spectroscopic properties of **5-9** are investigated in diluted CH_2Cl_2 solutions (c = 5.10^{-6} mol.L^{-1}, Fig. 4 and Table 1). **5a** displays absorptions bands with moderate extinction coefficient in the UV-Vis range (λ_{max} = 434 nm, ε = 2300 L. $mol^{-1}.cm^{-1}$). This absorption can be attributed to a π-π* transition with a small charge transfer (CT) character from the carbonyl to the conjugated cycles according to TD-DFT calculations (see electron density difference plot in Figure S32). Note that TD-DFT predicts a vertical absorption at 407 nm (*f*=0.15), slightly blueshifted as compared to the measured λ_{max}, a typical consequence of the neglect of vibronic couplings in the calculations. Interestingly, the most red-shifted absorption band displays negative solvatochromism (Fig. S20). This is consistent with the computed dipole moments of 5.61 and 2.64 D in the ground and excited states of **5a**, respectively. The effect of the R-group attached to the ketone is negligible (Fig. S19). Changing from exocyclic Ph to Cy also leads to minor modifications (Fig. 4). Changing to 6-membered P-rings leads to a gradual hyperchromic shift (**5a**-**7a**-**9**) of the most red-shifted transition. This hyperchromic effect is also found in theory that returns vertical absorption at 372 (*f*=0.24) and 401 nm (*f*=0.30) for **7a** and **9**, respectively. Obviously the trends in both position and intensities closely follows the experimental ones.

All compounds do not show fluorescence in diluted DCM solution (or only display very weak fluorescence). However, all derivatives featuring R_2= Ph display solid-state luminescence in the 550-600 nm area (Fig. S21) with moderate QY reaching ~20% for **5a** and **9** (Table 1).

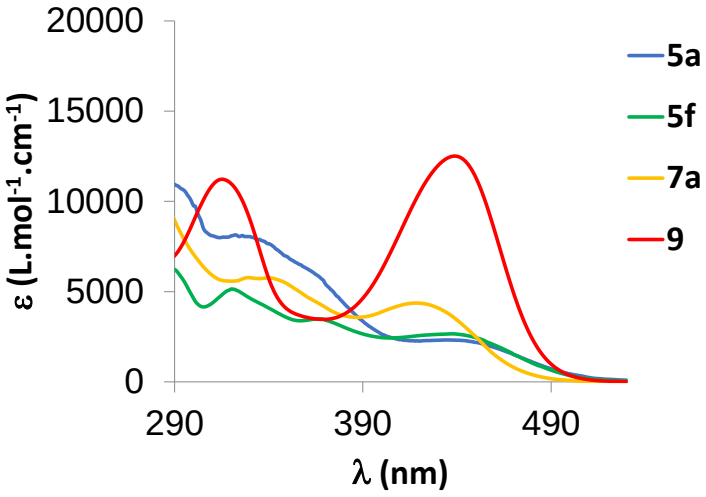

Figure 4: UV-vis absorption of **5a**, **5f**, **7a** and **9a** in diluted DCM solution (10^{-5} M).

The electrochemical behaviour of **5-9a** was investigated by cyclic voltammetry (CV) in dichloromethane solution (Figure S26-27 and Table 1). **5a-c**,**5f** display irreversible oxidations at low potential (for example E_{ox}(**5a**) = +0,16 V vs Fc^+/Fc), in agreement with the strong π-donating ability of the ylidic fragment.[26] As expected, insertion of electron-rich Cy exocyclic groups allows further decreasing the oxidation potential E_{ox}(**5f**) = +0,01 V vs Fc^+/Fc). While no reduction process is observed in **5a**, **5c** and **5f**, the insertion of electro-withdrawing groups in **5b** allows observing quasi-reversible reduction wave (E_{red} = -1.52 V vs Fc^+/Fc). Increasing the size of the P-ring from 5 to 6-members leads to an increase of the oxidation potential (for example E_{ox}(**7a**) = +0,23 V vs Fc^+/Fc). However, all these derivatives remain highly electron rich systems.

All those characterizations confirm that those P-containing acenaphthylenes and phenanthrenes display optical and redox properties that can be of interest in the context of plastic electronics or photonics. To go further with these systems, it is highly desirable to perform molecular engineering in order to optimize these properties or obtain new ones.

Absorption tuning.

Despite the presence of the ylidic bond, **7-9** show good thermal stability. We thus decided to test post-functionalization conditions, and in particular the direct arylation, which offers a straightforward diversification method directly on the C-H bonds.[27][28] In this context, thiophene-containing **9** appeared as an ideal platform. Using 5% $Pd(OAc)_2$ as catalyst, KOAc as base, in DMAc at 125°C, allowed preparing, in excellent yields, derivatives **10-11-12** featuring respectively electron-withdrawing or electron donating groups (Scheme 4). In addition, during the reaction with bromonitrobenzene, we could isolate the monoarylation product revealing that the first arylation occurs on the thiophene fused to the 2-3 position of the P-ring (compound **10'**, see ESI). **10** was additionally characterized by X-ray diffraction (Scheme 4) and the main structural characteristic described earlier remain valid.

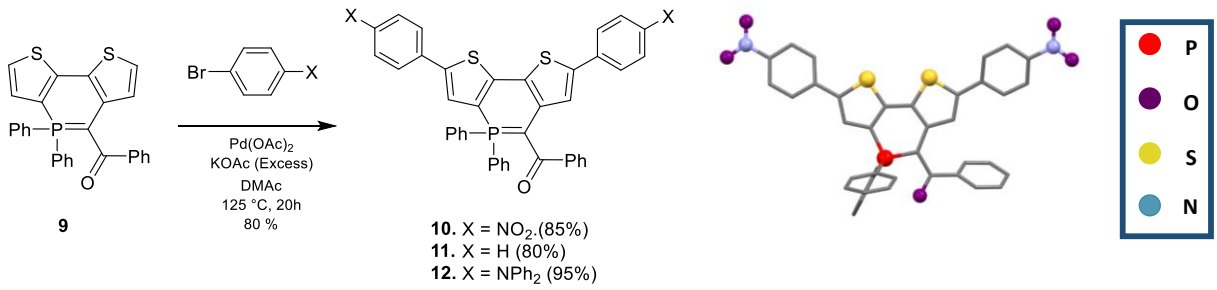

Scheme 4. Synthesis of **10-12** and X-ray structure of **10**.

The extension of the π-system and the insertion of electron rich/poor substituent leads to bathochromic and hyperchromic shifts (Fig. 5). **10-12** display absorption covering the visible range from 400 to 550 nm (ε_{max} ~ 27000 L. $mol^{-1}.cm^{-1}$). As anticipated by the electro-donating character of the ylidyl ring, the insertion of electron-poor nitroaryl groups in **10** leads to a redshifted absorption (λ_{abs} = 549 nm), whereas donor groups induce milder displacements. Similar trend is observed with the luminescence of the compounds (Table 1 and Fig. 5). While the absorption wavelengths are only weakly affected by the polarity of the solvent (Fig S22), all compounds display higher luminescence quantum yields in apolar solvent (pentane) with ϕ up to 50% for **10** and **12**. Interestingly, **11** and **12** also display solid-state emission in the red part of visible range. TD-DFT reproduces these trends with bright vertical absorption at 491, 439, and 451 nm for **10**, **11**, and **12**, respectively. Fluorescence wavelengths follow the same ordering (Table S3). We provide electron density difference plots for these three compounds in Fig. 6 and Fig S34. For **9**, there is an obvious CT from the core of the dye to the nitro group, confirming the electro-donating character of the ylidyl ring. In contrast, in both **11** and **12**, the side groups do not play any major role in the transition, explaining why these two compounds present alike spectral signatures.

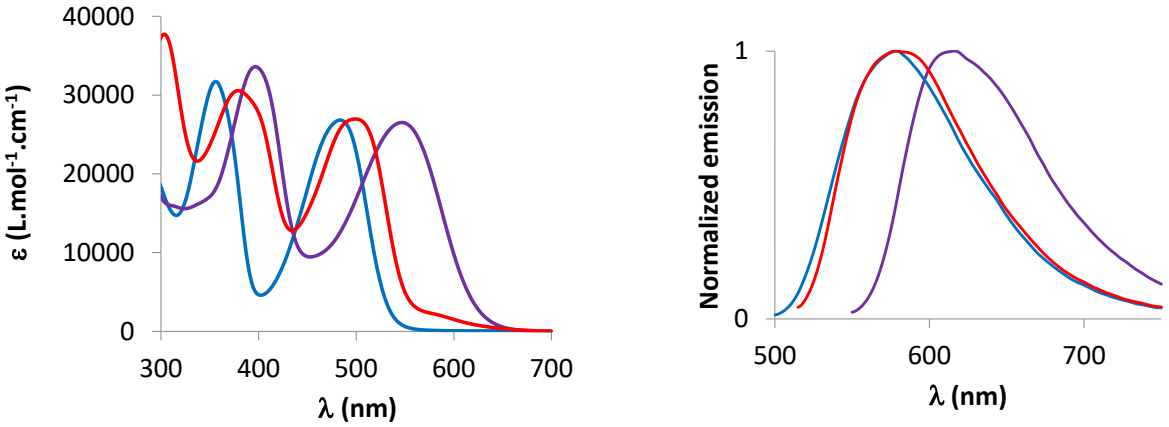

Figure 5. UV-vis absorption in DCM (5.10^{-5}M) (upper left) and emission in pentane (5.10^{-5}M) (upper right) of **10** (purple), **11** (blue), and **12** (red).

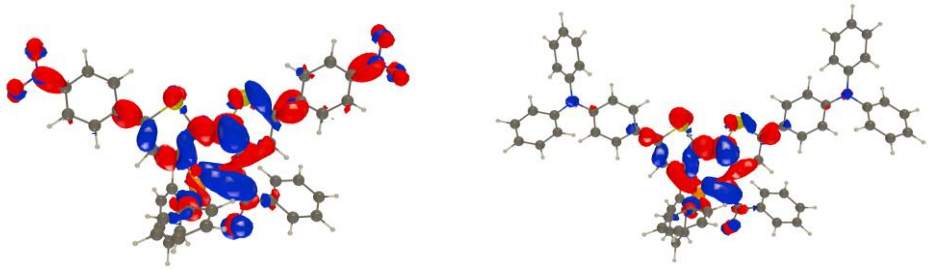

Figure 6. Density difference plots of **10** (left) and **12** (right). The blue and red lobes correspond to regions of decrease and increase of electron density upon excitation (absorption), respectively. Contour threshold: 1 x 10^{-3}.

The CV reveal that insertion of nitroaryl allows observing a quasi-reversible reduction (E_{red}(**9**) = -1.46 V vs Fc^{+}/Fc, Fig 7 and Table 1) in addition to the oxidation at low potential. **9** thus appears as an interesting derivative with amphoteric redox character and low band gap. The presence of electron rich substituents in addition to the ylidic ring in **10** and **11** (Eox_1) leads to the presence of multiple oxidation processes (E_{ox2}(11) = +0,81 V vs Fc^{+}/Fc; E_{ox2}(**12**) = + 0,30 V vs Fc^{+}/Fc, see Fig 5). However, the most electron rich part of the compound remain the cyclic ylide. These results illustrate the easy tuning of the HOMO-LUMO energies and thus the optical and redox properties, making these derivatives ideal synthon to build new generation of π-conjugated organophosphorus materials.

In order to further explore the photonic properties of these new dyes, the third order non-linear optical (NLO) properties of **12** were evaluated by the two-photon-absorption-induced fluorescence method in

hexane (see ESI). We show that **12** display two-photon absorption (2PA) in the near infrared with σ = 80 GM ±15% at 810 nm (see Fig. S24-25) as well as a very weak 2PA between 850 nm and 1000 nm (1 GM < σ < 5 GM ±15%). The main 2PA band is thus blue shifted compared to 2.λ_{max} (λ_{max} = 503 nm, Table 1). Theoretical calculations confirm that the S_0-S_1 transition has a very low σ of 6 GM, whereas the S_0-S_2 transition delivers a much larger two-photon response (96 GM according to TD-DFT, Table S4). This second band indeed shows a very strong CT nature, in contrast to the lowest one (Fig. S36), which is consistent with a high NLO response. Such NLO properties make thus these dyes attractive for various photonic application either in the field of material science (optical power limiting) or medicine (bio-imaging, phototherapy).

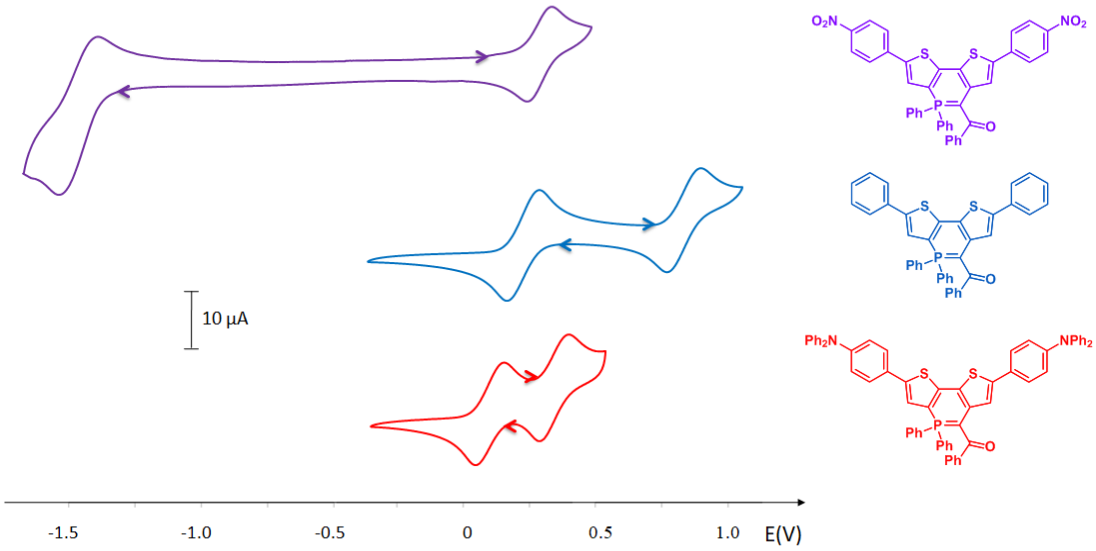

Figure 7: Cyclic voltammograms of **10-12** (c = 10^{-3} M) recorded in DCM (Bu_4NPF_6 (0.2 M), 200 mVs^{-1}, potentials vs Fc^+/Fc)(down).

Increasing the polyaromatic platform toward heteroacenes and heterohelicenes.

Polyaromatic systems, either linearly or helically arranged, nowadays play a key role in optoelectronic applications. It is thus of great interest to check if our synthetic approach allows introducing such scaffolds. The method appeared fully compatible for the efficient preparation of linear heteroacene **14** and of hetero[5]helicenes **16a-b** (Scheme 5).

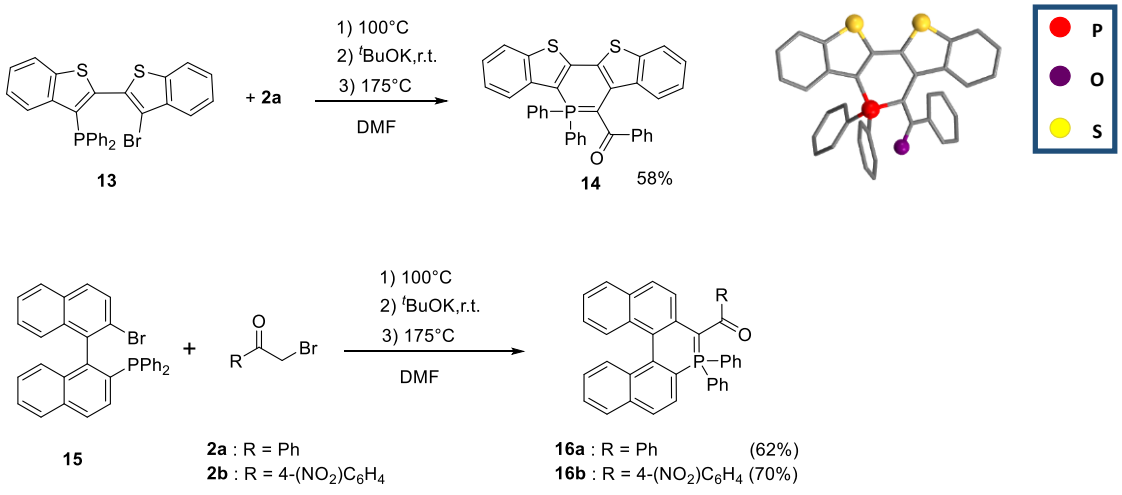

Scheme 5. Synthesis of phosphaacene **14** and phosphahelicene **16** and X-ray structure of **14**.

In particular, **16a-b** are the first examples of phosphahelicenes featuring an ylidic bond.[29] Enantiopure samples (with ee higher than 99%) of **16a** were obtained via HPLC over a chiral stationary phase (ESI). The enantiomerization barrier was determined, $\Delta G^{\neq}$ = 132.2 kJ.mol^{-1} at 132°C in chlorobenzene, (Fig. S30), 30 kJ.mol^{-1} higher than for [5]-carbohelicene[30], showing its high enantiomeric stability. Such behaviour was also previously observed with 7-membered P-ring based [5]helicenoïds, highlighting the pertinence of tuning helicenoïds with P-rings.[31] Such configurational stability allows studying the chiroptical of the λ^5-phosphahelicene. **16a** displays high specific optical rotations [(+)**16a**: α^{23}_D = + 346 ± 5%)) (c = 10^{-2} M, DCM). Electronic circular dichroism (ECD) was recorded in diluted DCM solutions. (+)**16a** and (-)**16a** displayed ECD with the expected mirror-image relationship (Fig. 7). (+)**16a** displays a strong positive ECD band ($\Delta\varepsilon$ = 75 at 272 nm), a negative band ($\Delta\varepsilon$ = -15 at 320 nm) and positive band ($\Delta\varepsilon$ = 8 at 398 nm). The spectra were nicely fitted by TD-DFT calculations (Figure **35**), which provides peaks with $\Delta\varepsilon$ of +104 at 291 nm, -43 at 345 nm, and +8 at 380 nm. This match enables the absolute configuration to be assigned as *P*-(+)/*M*-(–). In conclusion, those data confirm that λ^5-phosphahelicene **16a** exhibits the important chiroptical properties that make helicene unique and attractive for optoelectronic applications.

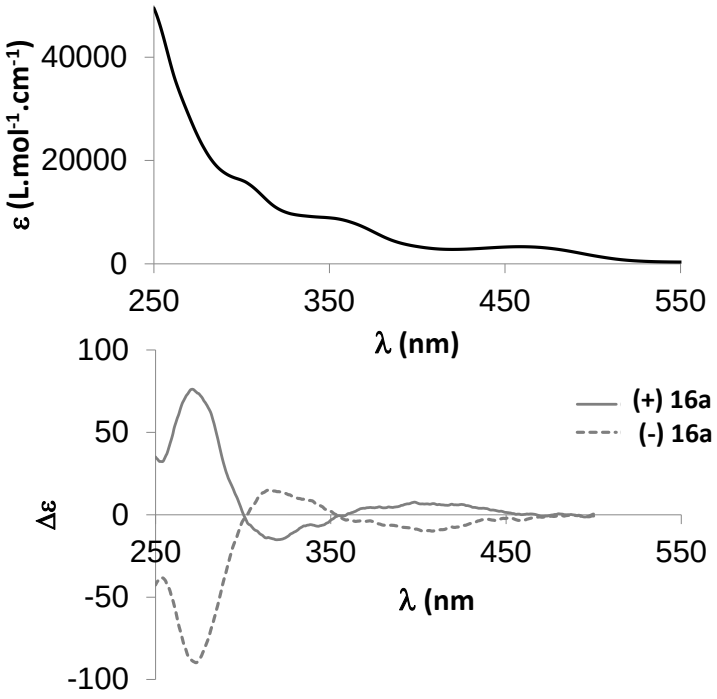

Figure 7: UV-vis absorption of **16a** and ECD spectra of (+)-**16a** (plain), (-)-**15a** (dotted) in DCM (10^{-5}M).

Table 1. Photophysical and redox data.

	λ_{abs} [a] [nm]	ε [a] [$M^{-1}cm^{-1}$]	$\lambda_{em(DCM)}$ [a] (ϕ) [b] [nm]	$\lambda_{em(C5)}$ [c] (ϕ) [b] [nm]	$\lambda_{emsolid}$ [d] (ϕ) [b,d] [nm]	E^{ox} [e] [V]	E^{red} [e] [V]
5a	434	2300	613 (1%)	602 (4%)	549 (25%)	0,16	-
5b	435	4700	-	-	-	0,25	-1,52[f]
5c	430	3700	-	-	574 (1%)	0,29	-
5f	436	2700	-	-	-	0,01	-
7a	419	4400	-	-	587 (2%)	0,23	-
7b	447	2000	-	-	-	0,39	-1,47f
9a	435	12500	-	-	584 (18%)	0,21 [f]	-
10	549	27000	-	616 (51%)	-	0,28[f]	-1,46[f]
11	485	27000	578 (<1%)	529 (32%)	632 (5%)	0,21 [f]	-
12	500	27000	608 (2%)	554 (48%)	649 (3%)	0,04 [f]	-
14	503	15000	629 (<1%)	621 (13%)	643 (12%)	0,19[f]	-
16a	460	3300	-	591 (8%)	608 (6%)	0,19[f]	
16b	462	5800	-	-	-	0,32 [f]	-1,48 [f]

[a] In CH_2Cl_2 (10^{-5}M). [b] Measured in calibrated integrated sphere. [c] In pentane (10^{-5}M). [d] measured in powder [e] In DCM with $Bu_4N^+PF_6^-$ (0.2 M) at a scan rate of 200 mV.s^{-1}. Potentials vs Fc^+/Fc. [f] Quasi-reversible process

In conclusion, a straightforward one-pot synthesis of 5 or 6-membered P-heterocycles featuring internal ylidic bond (P-containing acenaphthylenes and phenanthrenes) is presented (**5-9**). These π-conjugated systems are easily obtained through intramolecular cyclization of ylides, generated from readily available phosphines. Thanks to their chemical stability, these derivatives are easily post-functionalized through Pd-catalysed direct-arylation allowing the tuning of their absorption/emission on the entire visible range as well as their redox properties. Functional dyes with nonlinear optical properties can thus be prepared (**10-12**). In addition, the synthetic approach is also compatible with the preparation of polyaromatic derivatives, either linear (**14**) or helical (**16a-b**). The latter approach allowed preparing configurationally stable phospha[5]helicene with chiroptical properties. This article highlights the great potential of these novel organophosphorus derivatives synthesis method to prepare either more complex π-systems (higher helicenes, nanographenes etc) or functional dyes with applications in the field or organic electronics or photonics.

This work is supported by the Ministère de la Recherche et de l'Enseignement Supérieur, the CNRS, the Région Bretagne, the French National Research Agency (ANR Heterographene ANR-16-CE05-0003-01). This work used the computational resources of the CCIPL supercomputing center installed in Nantes.

[1] M. P. Duffy, W. Delaunay, P.-A. Bouit, M. Hissler, *Chem. Soc. Rev.* **2016**, *45*, 5296–5310.
[2] D. Joly, P.-A. Bouit, M. Hissler, *J Mater Chem C* **2016**, *4*, 3686–3698.
[3] T. Baumgartner, R. Réau, *Chem. Rev.* **2006**, *106*, 4681–4727.
[4] Y. Ren, T. Baumgartner, *Dalton Trans.* **2012**, *41*, 7792–7800.
[5] L. Nyulászi, T. Veszpremi, *J. Phys. Chem.* **1996**, *100*, 6456–62.
[6] G. Märkl, *Angew. Chem. Int. Ed. Engl.* **1963**, *2*, 479–479.
[7] K. Dimroth, in *Phosphorus-Carbon Double Bonds*, Springer Berlin Heidelberg, Berlin, Heidelberg, **1973**, pp. 1–147.
[8] G. Pfeifer, F. Chahdoura, M. Papke, M. Weber, R. Szűcs, B. Geffroy, D. Tondelier, L. Nyulászi, M. Hissler, C. Müller, *Chem. – Eur. J.* **2020**, *26*, 10534–10543.

[9] N. Hashimoto, R. Umano, Y. Ochi, K. Shimahara, J. Nakamura, S. Mori, H. Ohta, Y. Watanabe, Minoru. Hayashi, *J. Am. Chem. Soc.* **2018**, *140*, 2046–2049.
[10] B. S. B. Karunathilaka, U. Balijapalli, C. A. M. Senevirathne, Y. Esaki, K. Goushi, T. Matsushima, A. S. D. Sandanayaka, C. Adachi, *Adv. Funct. Mater.* **2020**, *30*, 2001078.
[11] B. S. B. Karunathilaka, U. Balijapalli, C. A. M. Senevirathne, S. Yoshida, Y. Esaki, K. Goushi, T. Matsushima, A. S. D. Sandanayaka, C. Adachi, *Nat. Commun.* **2020**, *11*, 4926.
[12] Y. Nishimura, Y. Kawamura, Y. Watanabe, M. Hayashi, *J. Org. Chem.* **2010**, *75*, 3875–3877.
[13] P. Federmann, H. K. Wagner, P. W. Antoni, J.-M. Moersdorf, J. L. Perez Lustres, H. Wadepohl, M. Motzkus, J. Ballmann, *Org. Lett.* **2019**, *21*, 2033–2038.
[14] G. Tao, F. Yang, L. Zhang, Y. Li, Z. Duan, F. Mathey, *Chin. Chem. Lett.* **2021**, *32*, 194–197.
[15] L. Zhang, F. Yang, G. Tao, L. Qiu, Z. Duan, F. Mathey, *Eur. J. Inorg. Chem.* **2017**, *2017*, 2355–2362.
[16] E. D. Matveeva, T. A. Podrugina, A. S. Pavlova, A. V. Mironov, A. A. Borisenko, R. Gleiter, N. S. Zefirov, *J. Org. Chem.* **2009**, *74*, 9428–9432.
[17] E. D. Matveeva, T. A. Podrugina, M. A. Taranova, D. S. Vinogradov, R. Gleiter, N. S. Zefirov, *J. Org. Chem.* **2013**, *78*, 11691–11697.
[18] E. D. Matveeva, D. S. Vinogradov, T. A. Podrugina, T. D. Nekipelova, A. V. Mironov, R. Gleiter, N. S. Zefirov, *Eur. J. Org. Chem.* **2015**, *2015*, 7324–7333.
[19] C. Müller, D. Wasserberg, J. J. M. Weemers, E. A. Pidko, S. Hoffmann, M. Lutz, A. L. Spek, S. C. J. Meskers, R. A. J. Janssen, R. A. van Santen, Dieter. Vogt, *Chem. - Eur. J.* **2007**, *13*, 4548–4559.
[20] J.-J. Hou, Y.-Z. Xu, Z.-J. Gan, X. Zhao, Z. Duan, F. Mathey, *J. Organomet. Chem.* **2019**, *879*, 158–161.
[21] H. Huang, Z. Wei, M. Wang, Z. Duan, F. Mathey, *Eur. J. Org. Chem.* **2017**, *2017*, 5724–5728.
[22] M. Hayashi, Y. Nishimura, Yutaka. Watanabe, *Chem. Lett.* **2017**, *46*, 1732–1735.
[23] S. Xu, H. Huang, Z. Yan, Q. Xiao, *Org. Lett.* **2019**, *21*, 10018–10022.
[24] F. Nief, C. Charrier, F. Mathey, M. Simalty, *Tetrahedron Lett.* **1980**, *21*, 1441–1444.
[25] H. Wang, W. Zhao, Y. Zhou, Z. Duan, F. Mathey, *Eur. J. Inorg. Chem.* **2011**, *2011*, 4585–4589.
[26] M. M. Burgoyne, T. M. MacDougall, Z. N. Haines, J. W. Conrad, L. A. Calhoun, A. Decken, C. A. Dyker, *Org. Biomol. Chem.* **2019**, *17*, 9726–9733.
[27] D. J. Schipper, K. Fagnou, *Chem. Mater.* **2011**, *23*, 1594–1600.
[28] T. Delouche, A. Mocanu, T. Roisnel, R. Szucs, E. Jacques, Z. Benko, L. Nyulaszi, P.-A. Bouit, Muriel. Hissler, *Org. Lett.* **2019**, *21*, 802–806.
[29] K. Dhbaibi, L. Favereau, J. Crassous, *Chem. Rev.* **2019**, *119*, 8846–8953.
[30] C. Goedicke, H. Stegemeyer, *Tetrahedron Lett.* **1970**, *11*, 937–940.
[31] R. Mokrai, A. Mocanu, M. P. Duffy, T. Vives, E. Caytan, V. Dorcet, T. Roisnel, L. Nyulászi, Z. Benkő, P.-A. Bouit, M. Hissler, *Chem. Commun.* **2021**, *57*, 7256–7259.